www.cadanda.com
Computer-Aided Design AND APPLICATIONS

# Extracting Grasping Cues from Pistol-Shaped Tools for Digital Human Models

Alexandre Macloud[1], Ali Zeighami[2], Rachid Aissaoui[3] and Louis Rivest[4]

[1]Dassault Systèmes, Montreal, Canada, alexandre.macloud@3ds.com
[2]Ecole de technologie supérieure, Université du Québec, ali.zeighami.1@ens.etsmtl.ca
[3]Ecole de technologie supérieure, Université du Québec, rachid.aissaoui@etsmtl.ca
[4]Ecole de technologie supérieure, Université du Québec, louis.rivest@etsmtl.ca

Corresponding author: Louis Rivest, louis.rivest@etsmtl.ca

**Abstract.** Instantiating a digital human model (DHM) in a scene to simulate a manufacturing task typically requires specifying how to grasp the necessary tools. This study proposes a method to automatically extract grasping cues from 3D models of tools. These cues are to be used as the input to determine a plausible task-oriented grasp for a DHM. This article focuses on extracting grasping cues from pistol-shaped tools such as pistol drills and pistol screwdrivers. These tools are considered here as having multiple directions as opposed to hammers or screwdrivers. The proposed method uses the tool's 3D geometry as the input. The geometry of the tool is analyzed iteratively to extract the main directions from the geometry. The main directions are the handle axis and the working (or body) axis. Once these main directions are obtained, the tool's geometry is scanned along an optimal direction to precisely identify the push trigger region. This method classifies tools' regions as their head, handle, and pistol trigger, thus reflecting each tool's affordance. The grasping cues are extracted from these regions to be used for generating a task-oriented grasp.

**Keywords:** Grasp, Grasping cues, Digital human model, Tool, Pistol-shaped tools, Trigger, Push trigger, Pistol Drill, Affordance, Segmentation.
**DOI:** https://doi.org/10.14733/cadaps.2021.1167-1185

## 1 INTRODUCTION

Instantiating a digital human model (DHM) in a scene to simulate a manufacturing task typically encompasses specifying a variety of aspects, such as the virtual manikin anthropometry, the 3D work environment as well as the tools involved in the task. The manikin should also grasp the tools in a plausible manner for a given task. To this end, the specified grasp should account for the tool's affordance as well as the task to simulate. The notion of object affordance is defined by Gibson [1] to refer to the actionable properties between the world and an actor (a person or

animal). In ergonomics, affordance makes it possible to make the use of an object or service "intuitive" to a user. Automatically specifying a plausible and task-oriented grasp remains a major challenge for digital human modeling.

To instantiate a DHM in a scene with minimum user input, Dassault Systèmes has developed a new virtual manikin posture solver called the Smart Posturing Engine (SPE) [2]. The SPE is intended to simulate and validate task feasibility in an industrial environment, such as automotive assembly lines, by automatically positioning a virtual manikin in a 3D scene. The grasping module of the SPE will automatically generate a plausible grasp for a given hand-held tool.

Tools have inherent affordance that lends to human action. Indeed, it is assumed that every tool possesses affordance features (or regions), such as a handle and a trigger (if any), that suggest how to interact with that tool for an expected task. Therefore, if one can analyze the tools' geometry to detect these affordance features, grasping cues could be extracted from them to devise a plausible grasp.

In our previous work (Macloud et al., [3]), we proposed a method to extract grasping cues from simple one-handed tools such as mallets, screwdrivers, pliers and straight drills. All these tools share the common characteristic of having one main direction, which is used when scanning the geometry to extract affordance features. We propose here a significant extension of this approach that allows the extraction of grasping cues from more complex geometries for tools that have multiple main directions, such as pistol drills and pistol screwdrivers, rather than a single direction.

The proposed method exploits the concepts of geometric feature extraction to iteratively determine an optimal direction for scanning the geometry of pistol-shaped tools. The geometric properties that allow the geometry to be segmented are extracted from section scans. Regions that are most useful to determine a plausible task-oriented grasp, such as the handle, the head and the push trigger are identified. Grasping cues are extracted according to the region type and finally fed to the SPE to generate plausible grasps.

The paper is organized as follows. We assess earlier works in this area in section 2, and detail the need for our approach. The proposed method is described in section 3. Section 4 presents an example and our validation results. Our conclusions are presented in section 5.

## 2 PREVIOUS WORK

Cutkosky and Howe [4] were amongst the first to classify the available approaches for grasping as analytical or data-driven. Analytical approaches refer to the methods that construct grasps by computing kinematic and dynamic equations of the hand and finger positions. Unfortunately, analytical approaches suffer from computational complexity, which prevents the resolution of task-oriented grasps [5, 6].

On the other hand, data-driven approaches open up new strategies by allowing detailed observations of either the object or human behavior [3]. According to Bohg & Kragic [7], data-driven grasp synthesis based on object observation can be classified into three groups based on what is assumed to be known a priori about the query object. Hence, a "Known Object" is an object that has been encountered before and for which grasps have already been generated. A "Familiar Object" assumes that the query object is similar to a previously encountered object. An "Unknown Object" corresponds to a new shape never grasped before. In the present paper, tools are considered as Familiar objects since they belong to a family that is assumed to be known before launching the analysis.

Data-driven approaches for object grasping for DHMs and robotics require the recognition of geometric features. During the past three decades, researchers have proposed different techniques to recognize geometric features, including segmentation-based approaches, neural network-based approaches, volume decomposition-based approaches and skeletonization [8]. All these methods

have their pros and cons and can be combined to leverage their respective strengths (as well as to compensate for their respective weaknesses).

Researchers have developed segmentation methods to extract geometric information, such as edges and smooth regions, from scanned data. For grasping purposes, El-Khoury et al. [9, 10] suggested that it is more appropriate to break down the query object into a set of functional regions than to analyze the object as a whole. The 3D mesh of an object is thus segmented into a set of elementary superquadrics and the most optimal region for grasping is then sought. Huang & Menq [11] proposed a systematic approach to automatically extract geometric surfaces from 3D point clouds by segmenting meshes, thanks to sharp and smooth border detection. More recently, Li et al. [12] proposed a powerful segmentation method based on volumetric eigenfunctions of the Laplace-Beltrami operator. Segmenting an object with a free form surface remains challenging when edges have small variations or when regions are homogeneous.

Artificial Neural Networks (ANNs) have been applied in the field of 3D feature recognition since the 1990s. Regarding grasping, Kyota et al. [13] proposed a method for point detection on geometric models. The detected points are then evaluated to determine if they are in a graspable portion or not by testing several candidate positions learned using a data glove. Prabhakar & Henderson [14] used ANN to recognize features from solid models. Schmidt et al. [15] presented a data-driven approach exploiting the Deep Convolutional Neural Network algorithm to resolve hand grasping posture for unknown objects. More recently, Zhang et al. [16] presented a novel framework of deep 3D convolutional neural network (3D-CNNs) called FeatureNet to learn machining features from CAD (Computer-Aided Design) models of mechanical parts. Overall, the use of neural networks requires a vast 3D geometry database, which limits the exploitation of machine learning for grasping.

Another approach used in geometric feature extraction is mesh skeletonization. Skeletons (see [17] for a thorough survey) can basically be defined as centered curvilinear structures that approximate the topology and geometry of 3D volumes. Skeletonization is a process that is mainly applied on polygonal meshes and volumetric models to retrieve mesh skeletons [18], [19], [20]. There is a vast literature of curve skeletons, starting with the well-known medial axis [21]. Diaz et al. [22] presented a feature extraction process to obtain grasping points oriented mainly to disassembly cooperative tasks from medial axis transform skeletonization. Meanwhile, Vahrenkamp et al. [23] proposed a grasp planner technique that integrates curve skeletonization and segmentation to generate robust grasps on the query object shape. Their results show that the skeleton-based grasp planner is able to autonomously generate high-quality grasps but does not provide a good skeleton for sharp edge geometries. Overall, skeletonization is a time-consuming process that sometimes lead to a lack of reliability due to the delicate balance between eliminating noise without overlooking small geometric details.

Globally, data-driven solutions for object grasping may combine segmentation, machine learning and skeletonization in order to provide better results for grasping unknown geometries [24], [10].

However, few methods have been proposed in the literature to help a virtual manikin to automatically determine how to grasp tools in a manufacturing environment. The work presented in our previous paper used a data-driven method combining segmentation and skeletonization notions [3] to extract affordance features from simple one-handed tools such as mallets, screwdrivers, pliers and straight drills, which have one main direction, and extract grasping cues from those features.

The present work proposes a method that allows extracting grasping cues from pistol-shaped tools that have multiple main directions, rather than a single direction. This paper presents two distinct contributions. First, it describes a method to determine the optimal scanning direction of the tool's geometry in order to efficiently recognize specific features (or regions) on the tool. Second, it presents a method to recognize specific affordance features, such as push triggers, found on this type of tools. The proposed method is described in the next section.

## 3 PROPOSED METHOD

### 3.1 General Approach

The general approach for extracting grasping cues was presented by Macloud et al. [3]. It focused on tools with a single main direction such as mallets, regular screwdrivers, pliers and straight drills, and highlighted a five steps method for extracting grasping cues (Figure 1, left).

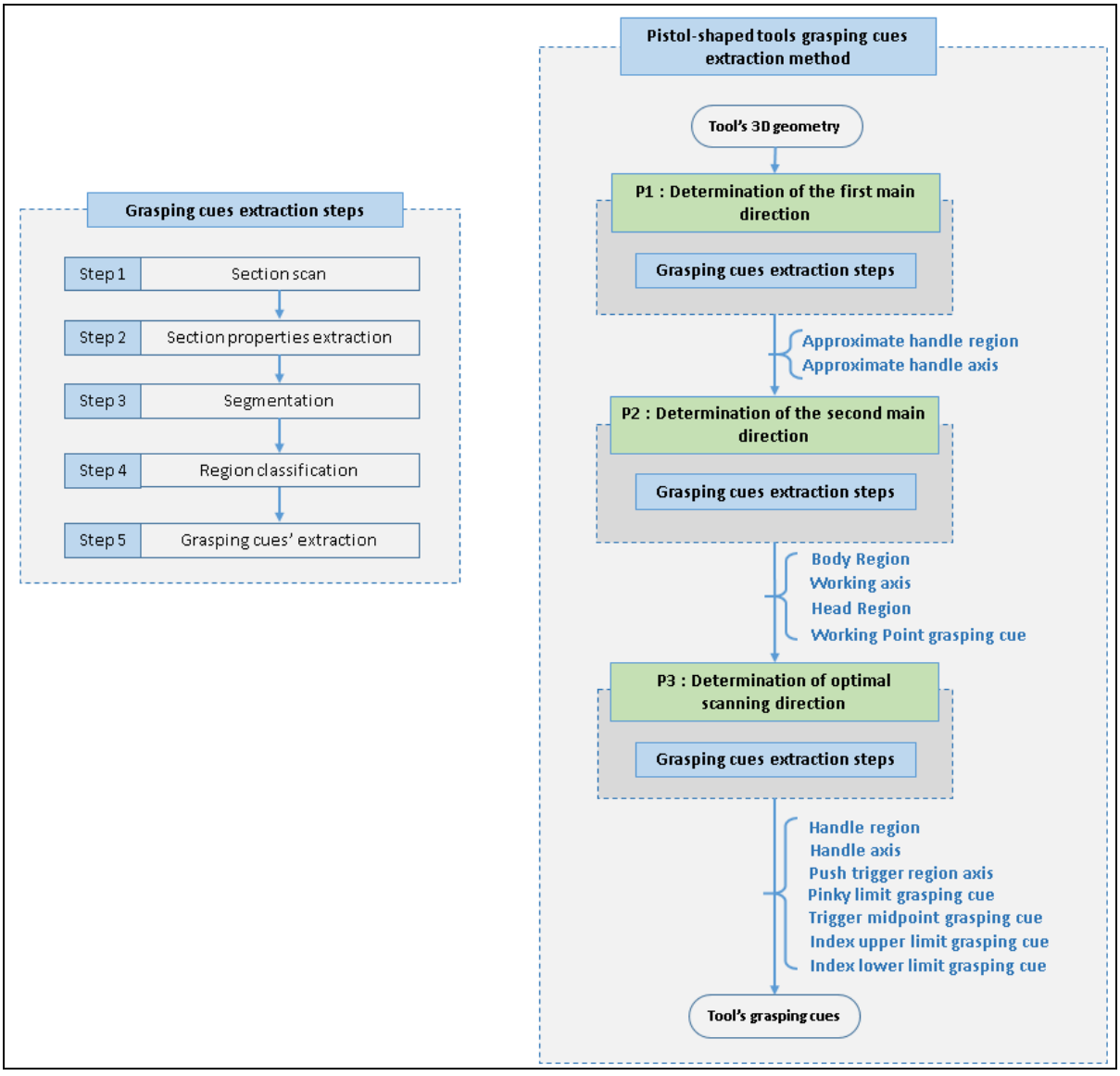


**Figure 1**: General process for extracting grasping cues.

First, a section scan was carried out on the 3D geometry of the tool to extract a series of sections, similar to the slicing described by Minetto et al. [25]. The scanning direction was obtained directly from the main direction of the oriented bounding box of the query tool [3]. The specific properties

were then extracted for each section. At the segmentation step, variations of sections' geometrical properties were analyzed so as to successively organize them into zones, segments, and regions. Next, the regions were classified and specific regions that influence the grasp, such as the handle, were identified. Finally, grasping cues were extracted from the identified regions, including the head of the tool that provides a working direction related to the task, as well as the handle or lever trigger, if any. Finally, these grasping cues were passed to the Smart Posturing Engine (SPE) to generate task-oriented grasps.

### 3.2 Pistol-Shaped Tools

Our method for extracting grasping cues from tools starts with the tool's 3D geometry. A wide variety of tools can be found on production lines. These tools generally have different geometries. The general approach described in Macloud et al. [3] and summarized above yielded excellent results for the tools in Figure 2, left. The present paper focuses on proposing an extended version of this approach for pistol-shaped tools, such as the drill shown in Figure 2, right.

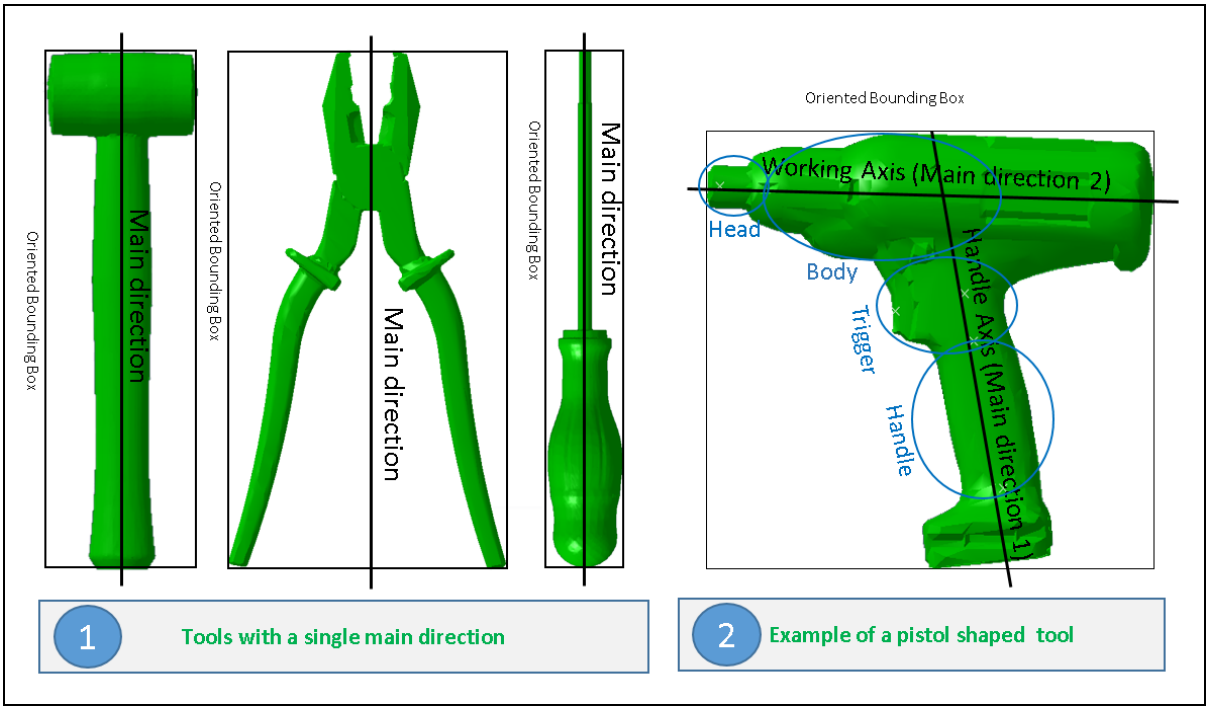


**Figure 2**: Tool types according to their main directions.

The tools belonging to the second type share two important characteristics: 1) their general shape is that of a pistol; and 2) they feature a push trigger. We consider here that the push trigger is a key affordance feature as it determines the position of the index finger on the tool. Hence, the proposed approach aims at identifying the trigger, as well as the other features mentioned above, of pistol-shaped tools.

However, push trigger detection remains challenging, as there is no specific criterion allowing it to always stand out from the rest of the segmented regions. This challenge is overcome by looking for the most typical region first. For example, in the 'mallet' family of tools, the most typical region was the head; therefore, for mallets, the head region was identified first. Hence, a predefined classification sequence is established for each tool family [3]. For pistol-shaped tools,

the identification sequence of affordance features is the following: Head → Handle → Trigger, as detailed later in this section.

The general approach presented above assumes that the direction of the scan performed in step 1 matches the main direction of the tool's bounding box. However, pistol-shaped tools do not satisfy this criterion. These tools are categorized here as 'tools with multiple main directions.' In this paper, pistol drills and pistol screwdrivers are considered. As illustrated in Figure 3, the overall shape of pistol drills and screwdrivers precludes direct use of the bounding box as an optimal scanning direction to precisely identify the trigger. In such a case, a series of steps, numbered P1 to P3 in Figure 1 (right), are used to determine the optimal scanning direction for identifying the push trigger.

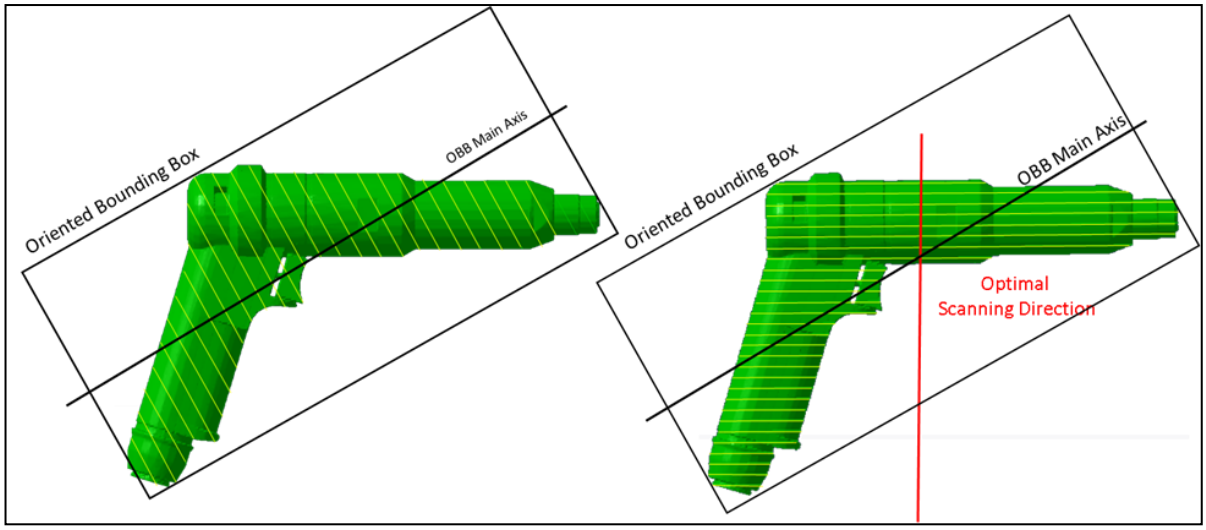


**Figure 3**: Oriented Bounding Box for pistol-shaped tools.

### 3.3 Optimal Scanning Direction

As mentioned above, a major key in determining a plausible grasp is to retrieve the push trigger. As explained in section 3.1 (General approach), the 3D geometry of the tool is scanned in order to identify the affordance features. The optimal scanning direction with which to identify the push trigger within pistol-shaped tools is perpendicular to the body axis, or working axis (Figure 2, right). This allows a significant change in face area to be generated at the transition from the handle/trigger regions to the tool body. This optimal scanning direction is obtained in three steps, P1, P2, P3, illustrated in Figure 4.

#### *3.3.1 Step P1: determining the first main direction*

For pistol-shaped tools, the first main direction corresponds to the handle axis. Hence, the first step, P1, searches for an approximate handle axis from the main axis of the bounding box. This handle region can be distinguished from the drill body thanks to its typical handle width, smaller than the body width. As per the general approach, a section scan is first performed along the main direction of the oriented bounding box and the properties are extracted for each section. Some 28 sections are set by default. When a face is included in another face, the inner face is removed. When two distinct faces are found in the same section, they are unified with the convex hull of the two faces. Sections are then organized in regions according to their area and GC (Geometric Center) variations. An approximate handle is then searched for among these regions by performing recognition tests, starting with the region of greatest height. The tested region parameters are compared to the values in Table 1. Since the orientation of the bounding box axis

is not assumed to be collinear with the handle axis, the properties of the regions are sometimes greater, and hence, the values associated with an approximate handle are larger than those of the actual handle (in Table 1). Moreover, in order to distinguish the handle from the body, we consider that the approximate handle region cannot be the one with the largest width of all the segmented regions, since the body is typically wider than the handle. Once the approximate handle region is identified, a singular value decomposition is used to generate an approximation of the handle axis passing through the average of the CGs of this region, arranged in a matrix of coordinates.

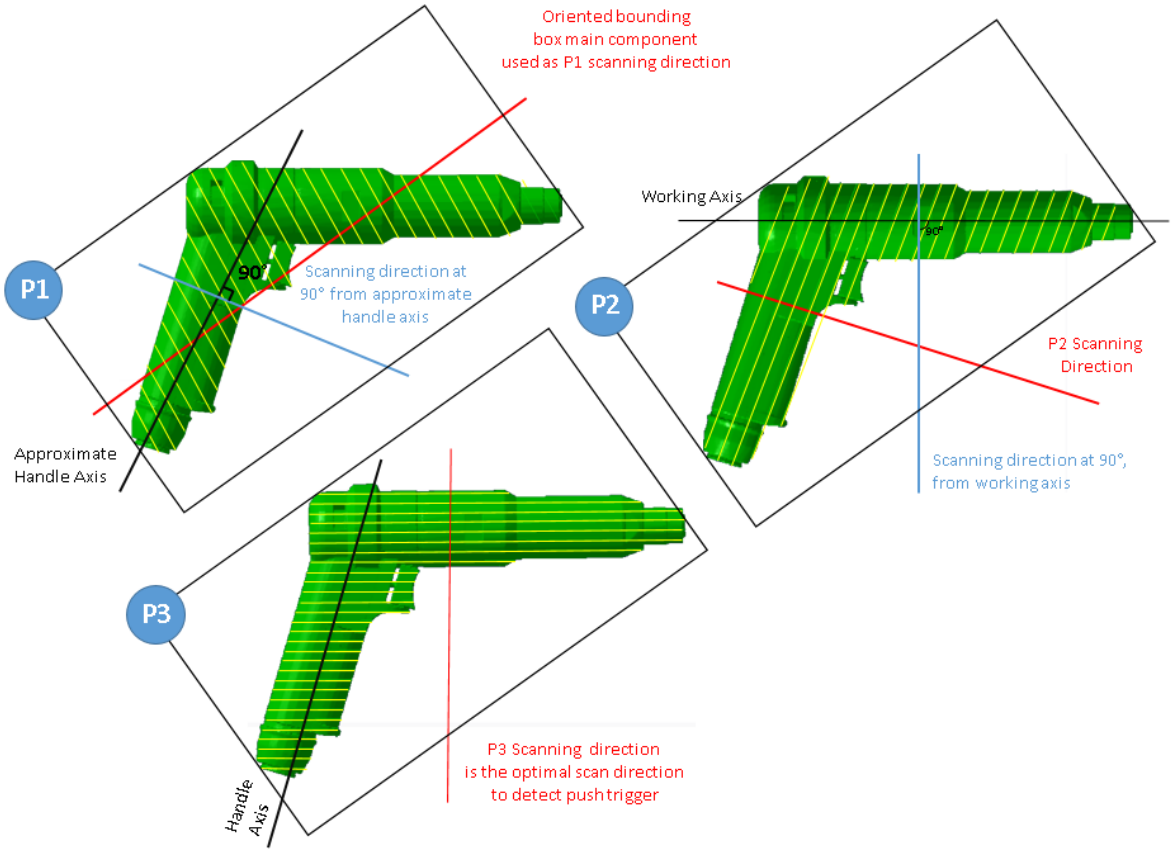


**Figure 4**: Illustration of steps P1, P2, P3 to determine the optimal scanning direction for push trigger detection.

### *3.3.2 Step P2: determining the second main direction*

For pistol-shaped tools, the second main direction corresponds to the working axis that passes through the tool's body. The second step, P2, consists of searching for this second main direction. For this purpose, a second scanning direction is oriented 90 degrees from the approximate handle axis identified in the previous step (Figure 4). This second section scan is performed with 19 sections. As before, when a face is included in another face, the inner face is removed. When two distinct faces are found in the same section, they are unified with the convex hull of those faces. Sections are then organized in regions based on the areas and GC variations. The body is then searched for among these regions by performing recognition tests, starting with the region of greatest height. The tested region parameters are compared to the values in Table 1. Moreover, in order to distinguish the body from the handle, we consider that the body region must have a greater width than the previously identified approximate handle, since the body is typically wider

than the handle. Once the body region is identified, a singular value decomposition is used to generate the working axis passing through the average of the GCs of the body region.

| | Max Area (mm²) | Min Area (mm²) | Max Height (mm) | Min Height (mm) | Max Width (mm) | Min Width (mm) | Region asymmetry |
|---|---|---|---|---|---|---|---|
| Approximate handle (Step P1) | 1600 | 250 | 350 | 50 | 60 | 30 | Not relevant |
| Body (Step P2) | 1600 | 300 | 350 | 50 | 60 | 30 | Not relevant |
| Handle (Step P3) | 1500 | 200 | 300 | 50 | 50 | 30 | Total symmetry or Partial asymmetry |
| Push Trigger (Step P3) | 1700 | 250 | 60 | 10 | 50 | 30 | Total asymmetry |

**Table 1**: Expected properties for pistol-shaped tool region classification.

Once the approximate handle axis and the working axis are known, the head of the tool (Figure 2, right) can be identified. This is done by comparing the width of a few extremum sections on both sides of the tool; the head is found on the side with the smallest width. The GC of the extremum face, for which the projected GC is the most distant to the approximate handle axis, is used as the working point of the tool's head needed as a grasping cue, as detailed in Macloud et al. [3]. It is worth noting that, while the tool's head is not grasped, it contributes to determining the grasp by orienting the tool toward the task to be performed.

#### *3.3.3 Step P3: determining the optimal scanning direction*

From the working axis identified at the previous step, we determine the optimal scanning direction for push trigger detection. Being perpendicular to the working axis, this scanning direction is considered optimal for identifying the push trigger region since it maximizes the variation of the section properties between the handle/trigger and body regions (Figure 4).

The steps remain the same as above. Sections are generated along the optimal scanning direction and their properties are extracted. Twenty-eight (28) sections are set by default. When a face is included in another face, the inner face is removed. When two distinct faces are found in the same section, they are unified with their convex hull.

In order to make it easier to identify the push trigger, the faces belonging to the body of the tool are first identified and then removed. Indeed, since the scanning is carried out in the direction perpendicular to the body of the tool, any section with an area greater than 2000 mm² is considered to be part of the tool's body and removed, this value having been empirically determined. Next, all the remaining sections are segmented into regions. A handle is then searched for by performing recognition tests on regions of greater heights. Once the handle is identified, the handle axis is obtained by performing a singular value decomposition on the GCs of the faces that belong to the handle region. This handle region and axis are used to search for the push trigger by its proximity to the handle region, as presented next.

### 3.4 Push Trigger Detection

A push trigger corresponds to an asymmetric region with a functional side where the index finger will be positioned. In order to identify the push trigger region, two properties, called 'Section Asymmetry' and 'Region Asymmetry' are evaluated, as described next.

### 3.4.1 Section asymmetry

This section asymmetry evaluation provides the information required to detect a push trigger. Indeed, as shown in Figure 5, a push trigger is associated with a change in the shape of the handle. Analyzing the evolution of section properties allows the identification of the trigger. Each section obtained in step 1 (Figure 1) consists of 'n' closed curves. Each closed curve is filled to form a face in step 2. The presence of a push trigger leads to a longer face length and a change in the positioning of the GC of the faces. By considering a distance L1 connecting the GC of the face to the Ex1 end, and with L2 its respective opposite distance to Ex2, it is assumed that a face is asymmetric if $|L1 - L2| > x$, where x is an empirically-fixed threshold of 1 mm.

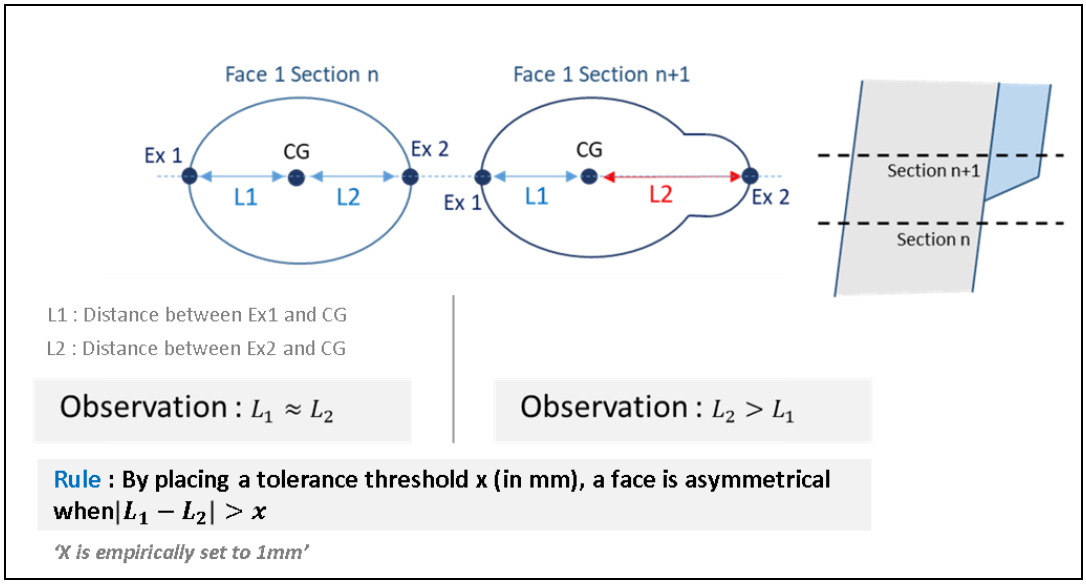


**Figure 5**: Section asymmetry.

### 3.4.2 Region asymmetry

As discussed in Macloud et al. [3], the evolution of section properties is exploited at the segmentation step (step 3, Figure 1, left) so as to organize the tool's geometry successively into zones, segments, and regions. A region is defined as a group of sections that share similar area and GC properties. Each region possesses elementary properties such as its height, width, length, GC and area. In the present paper, regions are also described by a new property, called region asymmetry. Region asymmetry is determined by analyzing the asymmetry of the faces belonging to the region. Three cases are considered:

- If more than 50% of the faces are asymmetrical and have a total height greater than 15mm, then the region is labeled as having 'Total asymmetry';
- If less than 50% of the faces are asymmetrical and have a total height less than 15 mm, then the region is labeled as having 'Total symmetry'; and
- Else the region is labeled as having 'Partial asymmetry'.

This region asymmetry property helps to detect push triggers, as discussed next.

### 3.4.3 Push trigger identification

At the beginning of step 4 (Figure 1, left), the tool geometry has been segmented into regions. Step 4 is where these regions are classified and identified as a head, a handle or a push trigger.

Since the head region was identified during the P2 step above, we now have to identify the handle and the push trigger.

The method used to identify the handle region was detailed in Macloud et al. [3]. To review, regions are identified by comparing their properties with the value range of the region type being searched. For example, a pistol drill handle is expected to have a width of between 30 and 50 mm, as shown in Table 1. Here, we assume that the handle region is already identified and we focus on identifying the push trigger region.

Depending on the segmentation parameters and the pistol-shaped tool geometry, three possible scenarios can arise (see Figure 6).

**Scenario 1 – Handle region with Total symmetry** (T.S. in Figure 6): A handle region was found and characterized by Total symmetry (Figure 6a and 6b, region C). Two situations can arise:

- Scenario 1a - The trigger identification step (to come) will identify a push trigger region (Figure 6d, region B); or
- Scenario 1b - The trigger identification step (to come) will not identify a push trigger region and so reenacts it (Figure 6e, region B).

**Scenario 2 – Handle region with Partial asymmetry** (P.A. in Figure 6): A handle region was found and characterized by Partial asymmetry (Figure 6c, region B). The trigger identification step (to come) will identify a push trigger region within this handle region.

Each scenario is analyzed as described below.

**Scenario 1a** - The push trigger region is identified in this scenario (Figure 6d). Starting from the first region above the handle, according to the distance from the tool's head (determined at step P2), the regions are tested successively according to the following two criteria:

- The region's properties' values fall within the values specified for push triggers in Table 1. Hence, the region must be labeled as having Total asymmetry, and its width must be between 30 and 50 mm; and
- For each asymmetric face of the region, one extremum point along the length must verify the rule $L_{exi} > \bar{L} + 5mm$, where $L_{exi}$ is the distance between the extremum point and the intersection of the handle axis with the face (P), while $\bar{L}$ characterizes the average distance between the extremum points and P for all faces of the handle region (Figure 7). This criterion verifies that the push trigger geometry includes a portion that is offset from the handle and that is where the index finger is positioned to operate the mechanism.

**Scenario 1b** - If at the previous step scenario 1a was not verified, no push trigger region was identified and scenario 1b applies. This scenario consists of reenacting the trigger. Thus, starting from the first section above the handle, in order of the distance from the head (determined at step P2), the sections are tested successively according to the following criteria:

- The section must be asymmetric; and
- Its corresponding face must verify the rule $L_{exi} > \bar{L} + 5mm$, as for scenario 1a above (Figure 7).

If the section does not qualify as belonging to the push trigger, it is discarded. If the section qualifies as belonging to the push trigger, it is counted and the test proceeds with the next section until a series of sections with a height of 20 mm is found; this series of sections is considered to be the push trigger region, illustrated as region B2 in Figure 6e. This process verifies that the push trigger region is at least 20 mm high and includes a portion that is offset at least 5mm from the handle axis and where the index finger can be positioned to operate the mechanism.

**Scenario 2** – Scenario 2 applies when a handle region was found and characterized by partial asymmetry. It is thus designed to retrieve, within that region, the asymmetric portion and the symmetric portion (Figure 6c). The symmetric portion of the region is expected to correspond to the handle (Figure 6f, region B1), whereas the asymmetric portion is tested as a push trigger according to the rules of scenario 1a (Figure 6f, region B2).

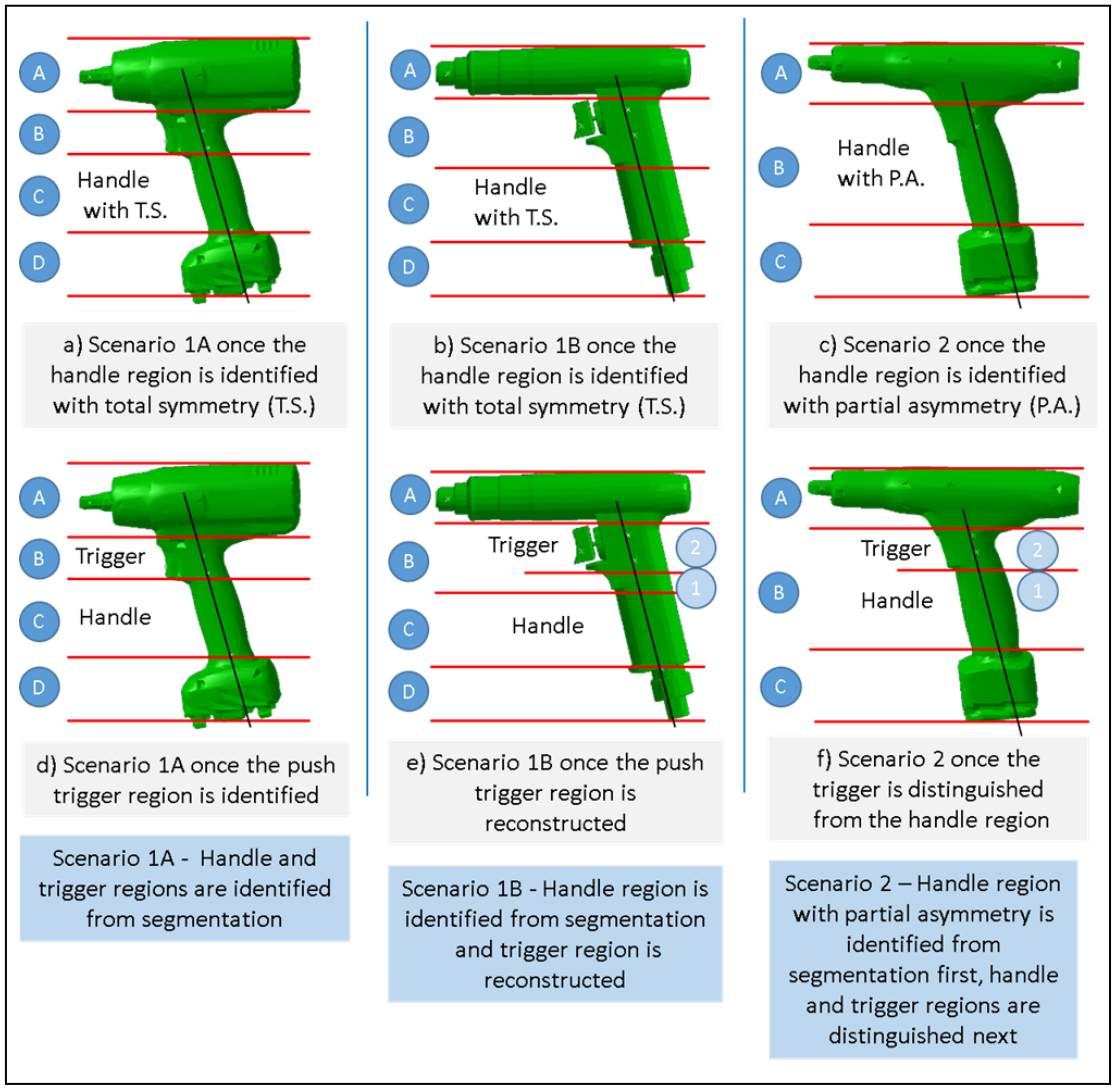


**Figure 6**: Scenarios for push trigger detection.

If none of these scenarios applies, then no trigger is identified. It can be noted, however, that in all of the tested cases a trigger was identified if a handle was identified.

### *3.4.4 Extraction of grasping cues for pistol-shaped tools*

For pistol-shaped tools, and as mentioned above, the affordance features are identified in sequence starting with the head, followed by the handle and finally the push trigger. The next step is to extract grasping cues from these features. The grasping cues associated with the head were extracted in step P2, just after identifying the head.

The handle axis was obtained in step P3 using a singular value decomposition to estimate a mean axis passing through the GCs of the faces belonging to the handle region. The two most distant faces of the handle region are used to determine the limits of the position of the hand on the handle. Precisely, the GCs of these two faces are projected on the handle axis to form the two

grasping cues that limit the hand translation: the pinky limit and the index limit. The index limit, however, will be replaced next by more precise cues extracted from the push trigger.

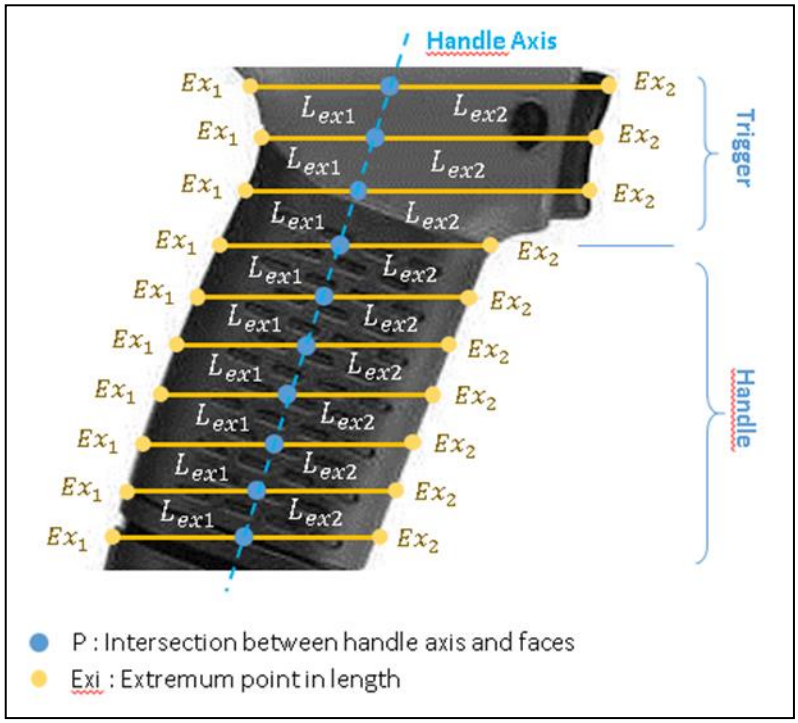


**Figure 7**: Push trigger faces' properties.

The grasping cues associated with the push trigger are obtained as follows. First, the functional side of the trigger is identified. The functional side is the side where the index finger will be positioned. It also is the side of the trigger that is the farthest from the handle axis. It is identified by projecting the extremum points (Ex1 and Ex2), obtained earlier (Figure 7), for each face of the trigger region onto the axis of the handle. The functional side is the side with the largest average projection distance. Once the functional side is identified, the position of the index on the trigger is conveyed by a grasping cue, designated as the 'Trigger Midpoint', calculated by averaging the extremum points of the functional side of the trigger region (Figure 8). Next, as it is possible for the index finger to move on the contact surface of the trigger, two index movement limits are conveyed by two grasping cues, the Index Upper Limit and the Index Lower Limit (Figure 8). These are calculated by projecting the extremum point belonging to the functional side of the first and last sections of the trigger region onto the handle axis. These grasping cues of the trigger and of the handle are illustrated in Figure 8.

## 4 PROPOSED METHOD ILLUSTRATION AND VALIDATION

In this section, we illustrate the proposed grasping cues extraction method on an example and present the results obtained from twelve industrial 3D CAD models.

### 4.1 Illustration of the Proposed Method in an Example

Since pistol-shaped tools have multiple main directions, successive section scans are performed.

**Step P1** aims at determining the tool's first main direction, which corresponds to the (approximate) handle axis. Hence, a first section scan of 28 sections is performed along the main axis of the OBB (the red line in Figure 4, P1), and the section properties are extracted. Inner faces are removed and distinct faces, if any, belonging to the same section are unified using their convex hull. The tool's 3D geometry is segmented according to the faces' area and the GC evolution. For the considered example, five regions are automatically generated, as shown in Figure 9 (P1, left). The regions' properties are provided in Table 2.

At this step, an approximate handle is searched for among the segmented regions. Regions are tested according to their decreasing height. Region 3 has the greatest height (154.5 mm), and its properties satisfy the requirements from Table 1. However, region 3 is also the widest of all the regions listed in Table 2 (33.4 mm). Since the width of the handle is expected to be smaller than the width of the body, region 3 is not identified as the handle region. Region 4 is tested next. Since its properties fall within the expected value ranges of an approximate handle (Table 1) while not being the widest segmented region (28.7 mm), this region is identified as the approximate handle. The approximate handle axis is obtained by performing a singular value decomposition on the GCs of the faces that belong to the approximate handle region.

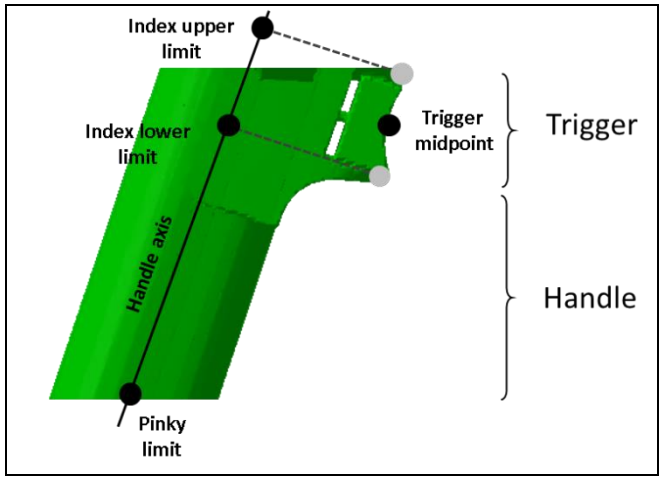


**Figure 8**: Trigger and handle grasping cues.

**Step P2** determines the tool's second main direction, which corresponds to the working axis that passes through the tool's body. The new scanning direction (the red line in Figure 4, P2) is obtained by rotating the approximate handle axis by 90 degrees around the smallest dimension of the bounding box. A section scan of 19 sections is performed and the section properties are extracted. Inner faces are removed and distinct faces, if any, belonging to the same section are unified using their convex hull. The tool's 3D geometry is segmented according to the evolution of the faces' area and of the GCs. For the considered example, six regions are automatically generated, as shown in Figure 9 (P2, center). The regions' properties are provided in Table 3.

At this step, the tool's body is searched for amongst the segmented regions. Regions are tested according to their decreasing height. Since the properties of region 2 fall between the expected value ranges of a body (Table 1), while having a greater width (33.2 mm) than the approximate handle (from the previous step, 28.7 mm), region 2 is identified as the body. The working axis is then obtained by performing a singular value decomposition on the GCs of the faces that belong to the body region.

During this step, the grasping cue corresponding to the tool's head is searched for by looking at the extremity of the smallest area. Its corresponding 'working point' is then extracted.

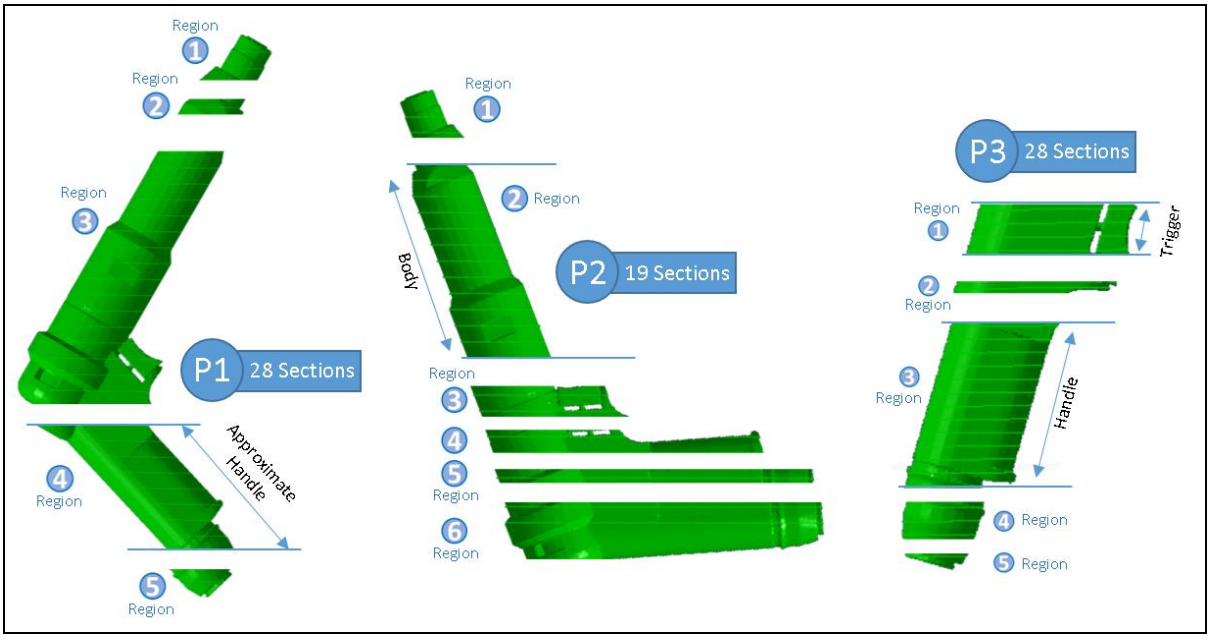


**Figure 9**: Segmentation results for the pistol-shaped drill illustrative example.

| Region Number | Region Area (mm²) | Region GC (mm) | Region Height (mm) | Region Width (mm) | Region asymmetry |
|---|---|---|---|---|---|
| 1 | 356.8 | (-13.26; 3.0; 0) | 14.4 | 15.1 | Total symmetry |
| 2 | 707.6 | (-29.0; 3.0; 0) | 0 | 27.1 | Total symmetry |
| 3 | 1521.2 | (-114.1; -10.6; 0) | 154.5 | 33.4 | Partial asymmetry |
| 4 | 1199.2 | (-201.8; -77.7; 0) | 82.8 | 28.7 | Total symmetry |
| 5 | 388.3 | (-228.8; -121; 0) | 0 | 24.9 | Total symmetry |

**Table 2**: Properties of regions obtained at step P1 for the pistol-shaped drill illustrative example.

**Step P3** aims at determining the optimal scanning direction with which to detect the push trigger. At this step, both main directions represented by the approximate handle axis and the working axis are known. The optimal direction (the red vertical line in Figure 4, P3) for this third section scan is obtained by rotating the body axis 90 degrees around the smallest dimension of the bounding box. A section scan of 28 sections is performed along this optimal direction and the section properties are extracted. Inner faces are removed and distinct faces, if any, belonging to the same section are unified using their convex hull. Moreover, to maximize the efficiency of trigger segmentation, sections with an area greater than 2000mm² are removed, as they are likely to belong to the body of the tool, which is useless at this step. The remaining (smaller) sections are organized according to the evolution of the faces' area and their GCs, as above.

| Region Number | Region Area (mm²) | Region GC (mm) | Region Height (mm) | Region Width (mm) | Region asymmetry |
|---|---|---|---|---|---|
| 1 | 412.7 | (-18.7; -1.4; 0) | 10.5 | 22.9 | Total symmetry |
| 2 | 980.2 | (-77.9; -0.8; 0) | 90.8 | 33.2 | Total symmetry |
| 3 | 1739.3 | (-142.9; -15.4; 0) | 13.1 | 36.4 | Total asymmetry |
| 4 | 2387.5 | (-173.7; -59.6; 0) | 0 | 8.6 | Total asymmetry |
| 5 | 4101.1 | (-191.0; -80.9; 0) | 0 | 8.8 | total asymmetry |
| 6 | 5064.5 | (-191.6; -46.7; 0) | 9.2 | 29.3 | Total asymmetry |

**Table 3**: Properties of regions obtained at step P2 for the pistol-shaped drill illustrative example.

| Region Number | Region Area (mm²) | Region GC (mm) | Region Height (mm) | Region Width (mm) | Region asymmetry |
|---|---|---|---|---|---|
| 1 | 1497.1 | (-169.3; -16.9; 0) | 16.5 | 20.4 | Total asymmetry |
| 2 | 1597.2 | (-183; -44.1; 0) | 0 | 28.4 | Total asymmetry |
| 3 | 998.5 | (-202.3; -78.9; 0) | 62.3 | 28.6 | Total symmetry |
| 4 | 728.5 | (-219.2; -116.2; 0) | 5.1 | 30.1 | Total symmetry |
| 5 | 634.4 | (-221.6; -124.9; 0) | 0 | 27.9 | Total symmetry |

**Table 4**: Properties of regions obtained at step P3 for the pistol-shaped drill illustrative example.

For the given example, five regions are automatically generated, as shown in Figure 9, P3. These regions' properties are provided in Table 4.

At this step, the handle is searched for amongst the segmented regions. The regions are tested in order of their decreasing height. Region 3 has the greatest height (62.3 mm), and its properties satisfy the requirements from Table 1 for a handle. The handle axis is obtained by performing a singular value decomposition on the GCs of the faces that belong to this handle region.

Since the handle region identified above is labeled as having Total symmetry, searching for the push trigger is done according to scenario 1. Regions are tested iteratively, starting from the first region above the handle, according to the distance from the tool's head. Region 2 is tested first here, but its height is null, and so it cannot be identified as a trigger (the height is null because the region counts only one section). Region 1 is tested next. Its properties satisfy the specifications for a push trigger in Table 1, and all four sections of the region have one extremum point that

satisfies the rule $L_{axi} > \bar{L} + 5mm$. Hence, scenario 1a prevails and region 1 is identified as the trigger region.

The very last step is to extract the grasping cues (Figure 10). For the handle, the GCs of the two most distant faces of the handle region are projected on the handle axis to form the two grasping cues that limit the hand translation on the handle axis: the pinky limit and the index limit. The index limit, which is closer to the trigger, is disregarded, to be replaced by more precise cues from the trigger. For the trigger, the trigger midpoint cue is calculated by averaging the extremum points belonging to the functional side of the trigger region. Next, the extremum points on the functional side of the trigger of the two most distant faces of the trigger region are projected on the handle axis to form the two grasping cues that limit the index translation, yielding the index upper limit and the index lower limit. All of these grasping cues are shown in Figure 10.

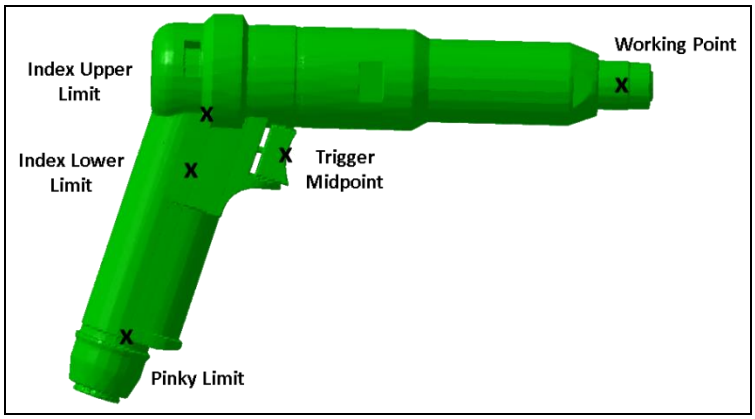


**Figure 10**: Grasping cues obtained for the pistol-shaped drill illustrative example.

### 4.2 Test Results and Discussion

This grasping cues extraction method was tested on twelve pistol-shaped tools (using electric or pneumatic power) retrieved from Part Supply, a catalog of sourceable 3D components, or from GrabCAD, a collaboration environment that allows the sharing of CAD models. The grasping cues obtained for ten of these pistol-shaped tools were quite satisfactory, as shown in Figure 11.

Determining if the grasping cues are satisfactory, or not, is based on a human's expected grasp of the tool. If the grasping cues are visually positioned in a plausible way, then the result is considered valid. Otherwise, the result is considered incorrect.

Two of the twelve tested tools yielded no result because their general shape was too different from a typical pistol shape. In one of these cases (Number 12, Figure 11) the geometry of the body is too small to allow the reconstruction of an adapted working axis at step P2. Hence, no optimal scanning direction could be determined. In the other case (Number 11, Figure 11), the square clutch at the rear of the body inhibits the identification of the approximate handle region in step P1.

It would have been useful to conduct a greater number of tests to further validate the method. It has proved challenging, however, to collect a large number of 3D CAD models of adequate quality. As mentioned above, all of the models tested here were retrieved from Part Supply or from GrabCAD. While other online platforms, such as TurboSquid or Sketchfab, also offer a variety of 3D models freely shared by Internet users, these models do not come from industrial sources, but from other fields such as computer graphics, for which the design constraints are different. Hence, the results would have had questionable validity.

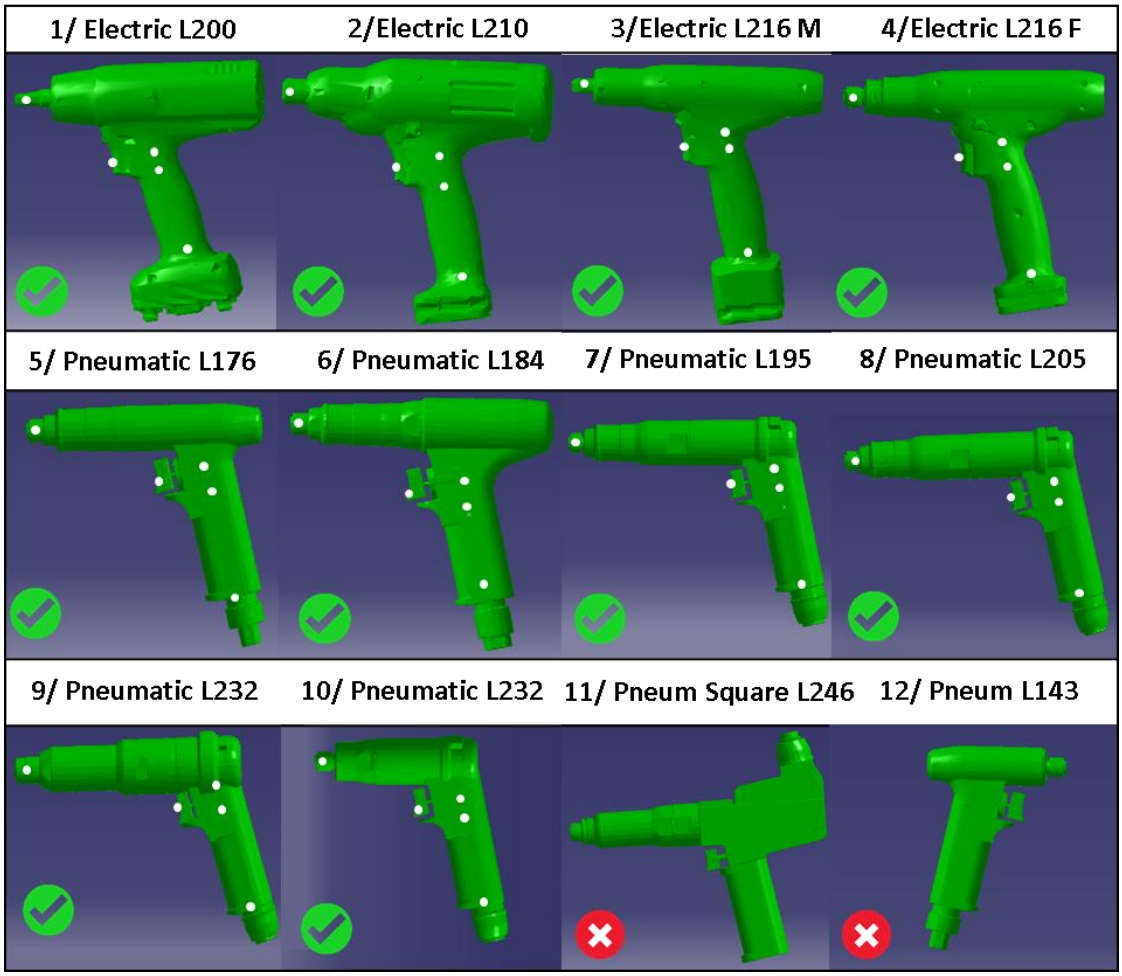


**Figure 11**: Grasping cues obtained for 12 pistol-shaped tools.

In addition, the proposed method relies on the scanning of the 3D geometry and leads to the extraction of sections. Indeed, the larger the step size (or the distance between sections), the greater the risk of missing a shape variation. On the other hand, too fine a scanning step would not allow the detection of large but continuous variations. One possible solution would be to perform two scans: a coarser one to detect transitions between regions, and a finer one to refine data acquisition where necessary.

Finally, the proposed method recognizes features (a body, handle, push trigger) based on the assumption that the family of tools to which the analyzed CAD model belongs is known beforehand, so that it can look for those features. This implies a limitation that the proposed algorithm, as described, only works for pistol drills and pistol screws, considered as a family. However, that family encompasses many individual tools, and so the proposed method is likely to make a significant contribution. Moreover, the proposed algorithm is composed of many different elements, such as push trigger recognition, that are likely to be reused with other families of tools.

## 5 CONCLUSION

This study has proposed the only method, to the authors' knowledge, that allows automatically extracting grasping cues from 3D CAD models of pistol-shaped tools. In our previous paper, a method was described for tools in which the scanning direction was directly obtained from the CAD model's oriented bounding box, as is the case for mallets, pliers or screwdrivers [3]. In the present study, we built on our previous work to propose a method that automatically determines the optimal scanning direction for pistol-shaped tools (which have a more complex geometry than mallets, for example), and that leads to identifying the push trigger as a key affordance feature.

This method encompasses three steps (P1, P2, and P3) whose objective is to determine the main directions of the tool. First (P1), the approximate handle region and approximate handle axis are determined. Second (P2), the approximate handle axis is used to determine the tools' body region and working axis. Third (P3), the working axis is utilized to determine the optimal scanning direction to identify the push trigger region.

The general process includes the same 5 steps for each scanning direction. First, a section scan is performed. Second, the section properties are extracted, including new properties called section asymmetry and region asymmetry, that are used to identify the push trigger. Third, the 3D geometry is segmented into zones, segments, and regions. Fourth, the regions that are meaningful for grasping are identified, and fifth, grasping cues are extracted for each type of region. The proposed method was validated on a dozen CAD models of professional quality. The grasping cues were successfully extracted on all ten of these for which the tool actually had a typical pistol shape.

*Alexandre Macloud*, http://orcid.org/0000-0001-6571-7529
*Ali Zeighami*, http://orcid.org/0000-0002-1890-8258
*Rachid Aissaoui*, http://orcid.org/0000-0001-7843-1386
*Louis Rivest*, http://orcid.org/0000-0003-0112-0090

## REFERENCES

[1] Gibson, J.J.; The theory of affordances, Hilldale, USA, 1977.
[2] Lemieux, P.O.; Barré, A.; Hagemeister, N.; Aissaoui, R.; Degrees of freedom coupling adapted to the upper limb of a digital human model, International Journal of Human Factors Modelling and Simulation, 5(4), 2017, 314-337. https://doi.org/10.1504/IJHFMS.2017.087015
[3] Macloud, A.; Zeighami, A.; Aissaoui, R.; Rivest, L.; Extracting grasping cues from one-handed tools geometry for digital human models, International Conference on Human Systems Integration (HSI2019), Biarritz, France, 2019.
[4] Cutkosky, M.R.; Howe, R.D.; Human grasp choice and robotic grasp analysis, in Dextrous robot hands, pp. 5-31, Springer, New York, NY, 1990. https://doi.org/10.1007/978-1-4613-8974-3_1
[5] Bohg, J.; Morales, A.; Asfour, T.; Kragic, D.; Data-driven grasp synthesis—a survey, IEEE Transactions on Robotics, 30(2), 2013, 289-309. https://doi.org/10.1109/TRO.2013.2289018
[6] Nguyen, V.D.; Constructing force-closure grasps, The International Journal of Robotics Research, 7(3), 1988, 3-16. https://doi.org/10.1177/027836498800700301
[7] Bohg, J.; Kragic, D.; Learning grasping points with shape context, Robotics and Autonomous Systems, 58(4), 2010, 362-377. https://doi.org/10.1016/j.robot.2009.10.003
[8] Rouhi, R.; Amiri, M.; Irannejad, B.; A review on feature extraction techniques in face recognition, Signal & Image Processing, 3(6), 2012, 1. https://doi.org/10.5121/sipij.2012.3601
[9] Sahbani, A.; El-Khoury, S.; Bidaud, P.; An overview of 3D object grasp synthesis algorithms, Robotics and Autonomous Systems, 60(3), 2012, 326-336. https://doi.org/10.1016/j.robot.2011.07.016

[10] El-Khoury, S.; Sahbani, A.; A new strategy combining empirical and analytical approaches for grasping unknown 3D objects, Robotics and Autonomous Systems, 58(5), 2010, 497-507. https://doi.org/10.1016/j.robot.2010.01.008
[11] Huang, J.; Menq, C.H.; Automatic data segmentation for geometric feature extraction from unorganized 3-D coordinate points, IEEE Transactions on Robotics and Automation, 17(3), 2001, 268-279. https://doi.org/10.1109/70.938384
[12] Li, X.; Zhang, Y.J.; Yang, X.; Xu, H.; Xu, G.; Point cloud surface segmentation based on volumetric eigenfunctions of the Laplace-Beltrami operator, Computer Aided Geometric Design, 71, 2019, 157-175. https://doi.org/10.1016/j.cagd.2019.03.004
[13] Kyota, F.; Watabe, T.; Saito, S.; Nakajima, M.; Detection and evaluation of grasping positions for autonomous agents, in 2005 International Conference on Cyberworlds (CW'05), IEEE, 2005, pp. 8 pp. https://doi.org/10.1109/CW.2005.39
[14] Prabhakar, S.; Henderson, M.R.; Automatic form-feature recognition using neural-network-based techniques on boundary representations of solid models, Computer-Aided Design, 24(7), 1992, 381-393. https://doi.org/10.1016/0010-4485(92)90064-H
[15] Schmidt, P.; Vahrenkamp, N.; Wächter, M.; Asfour, T.; Grasping of unknown objects using deep convolutional neural networks based on depth images, in 2018 IEEE International Conference on Robotics and Automation (ICRA), IEEE, 2018, 6831-6838. https://doi.org/10.1109/ICRA.2018.8463204
[16] Zhang, Z.; Jaiswal, P.; Rai, R.; FeatureNet: Machining feature recognition based on 3D convolution neural network, Computer-Aided Design, 101, 2018, 12-22. https://doi.org/10.1016/j.cad.2018.03.006
[17] Cornea, N.D.; Silver, D.; Min, P.; Curve-skeleton properties, applications, and algorithms, IEEE Transactions on visualization and computer graphics, 13(3), 2007, 530-548. https://doi.org/10.1109/TVCG.2007.1002
[18] Au, O.K.C.; Tai, C.L.; Chu, H.K.; Cohen-Or, D.; Lee, T.Y.; Skeleton extraction by mesh contraction, in: ACM transactions on graphics (TOG), 27(3), 2008, 1-10. https://doi.org/10.1145/1360612.1360643
[19] Ma, C.M.; Wan, S.Y.; Lee, J.D.; Three-dimensional topology preserving reduction on the 4-subfields, IEEE Transactions on Pattern Analysis and Machine Intelligence, 24(12), 2002, 1594-1605. https://doi.org/10.1109/TPAMI.2002.1114851
[20] Svensson, S.; Nyström, I.; Di Baja, G.S.; Curve skeletonization of surface-like objects in 3D images guided by voxel classification, Pattern Recognition Letters, 23(12), 2002, 1419-1426. https://doi.org/10.1016/S0167-8655(02)00102-2
[21] Holleman, C.; Kavraki, L.E.; A framework for using the workspace medial axis in PRM planners, in Proceedings 2000 ICRA. Millennium Conference. IEEE International Conference on Robotics and Automation. Symposia Proceedings (Cat. No. 00CH37065), IEEE, Vol 2, 2000, 1408-1413. https://doi.org/10.1109/ROBOT.2000.844795
[22] Díaz, C.; Puente, S.; Torres, F.; Grasping points for handle objects in a cooperative disassembly system, IFAC Proceedings Volumes, 40(2), 2007, 112-117. https://doi.org/10.3182/20070523-3-ES-4907.00020
[23] Vahrenkamp, N.; Koch, E.; Wächter, M.; Asfour, T.; Planning high-quality grasps using mean curvature object skeletons, IEEE Robotics and Automation Letters, 3(2), 2018, 911-918. https://doi.org/10.1109/LRA.2018.2792694
[24] Berscheid, L.; Rühr, T.; Kröger, T.; Improving Data Efficiency of Self-supervised Learning for Robotic Grasping, In 2019 International Conference on Robotics and Automation (ICRA), IEEE, 2019, 2125-2131. https://doi.org/10.1109/ICRA.2019.8793952
[25] Minetto, R.; Volpato, N.; Stolfi, J.; Gregori, R.M.; Da Silva, M.V.; An optimal algorithm for 3D triangle mesh slicing, Computer-Aided Design, 92, 2017, 1-10. https://doi.org/10.1016/j.cad.2017.07.001